Cytoplasmic localization of SETDB1-induced Warburg effect via c-MYC-LDHA axis enhances migration and invasion in breast carcinoma

WENLIN YANG[1*], YINGZE WEI[1*], TING WANG[2*], YING XU[2], XIAOXIA JIN[1], HONGYAN QIAN[1], SHUYUN YANG[1] and SONG HE[1]

[1]Department of Pathology, Nantong Tumor Hospital Affiliated to Nantong University, Nantong, Jiangsu 226006; [2]Department of Pathology, Affiliated Hospital of Jining Medical University, Jining, Shandong 272029, P.R. China

Received October 20, 2023; Accepted January 31, 2024

DOI: 10.3892/ijmm.2024.5364

Abstract. SET domain bifurcated 1 (SETDB1), a pivotal histone lysine methyltransferase, is transported to the cytoplasm via a chromosome region maintenance 1 (CMR1)-dependent pathway, contributing to non-histone methylation. However, the function and underlying mechanism of cytoplasmic SETDB1 in breast cancer remain elusive. In the present study, immunohistochemistry revealed that elevated cytoplasmic SETDB1 was correlated with lymph node metastasis and more aggressive breast cancer subtypes. Functionally, wound healing and Transwell assays showed that cytoplasmic SETDB1 is key for cell migration and invasion, as well as induction of epithelial-mesenchymal transition (EMT), which was reversed by leptomycin B (LMB, a CMR1 inhibitor) treatment. Furthermore, RNA-seq and metabolite detection revealed that cytoplasmic SETDB1 was associated with metabolism pathway and elevated levels of metabolites involved in the Warburg effect, including glucose, pyruvate, lactate and ATP. Immunoblotting and reverse transcription-quantitative PCR verified that elevation of cytoplasmic SETDB1 contributed to elevation of c-MYC expression and subsequent upregulation of lactate dehydrogenase A (LDHA) expression. Notably, gain- and loss-of-function approaches revealed that LDHA overexpression in T47D cells enhanced migration and invasion by inducing EMT, while its depletion in SETDB1-overexpressing MCF7 cells reversed SETDB1-induced migration and invasion, as well as the Warburg effect and EMT. In conclusion, subcellular localization of cytoplasmic SETDB1 may be a pivotal factor in breast cancer progression. The present study offers valuable insight into the novel functions and mechanisms of cytoplasmic SETDB1.

Correspondence to: Professor Shuyun Yang or Professor Song He, Department of Pathology, Nantong Tumor Hospital Affiliated to Nantong University, 30 Tongyang North Road, Tongzhou, Nantong, Jiangsu 226006, P.R. China
E-mail: yangsy123648@163.com
E-mail: hesong515@sina.com

*Contributed equally

Key words: breast cancer, migration, invasion, epithelial-mesenchymal transition, Warburg effect, SET domain bifurcated 1, c-MYC, lactate dehydrogenase A

Introduction

Breast cancer (BC) is one of the most frequently diagnosed cancers globally and ranks as the leading cause of cancer-related mortality in female patients, with an estimated 2.3 million new cases in 2020 (1). Metastatic (M)BC is characterized by an incurable nature and 53.3% overall survival (OS) rate at 5 years and has limited effective treatment options (2). Consequently, identification of crucial molecular targets implicated in metastasis holds promise for the formulation of novel therapeutic strategies tailored to patients with MBC. SET domain bifurcated 1 (SETDB1), belonging to the histone H3 lysine 9 methyltransferase (HKMT) family, serves a role in gene silencing via catalytic H3K9 methylation (3,4). Numerous studies have identified SETDB1 as an oncogene linked to metastasis and unfavorable prognosis in various solid tumors, including non-small cell lung cancer (NSCLC) (5,6), hepatocellular carcinoma (7), melanoma (8) and BC (9). Notably, SETDB1 amplification is detected in 9.1% of BC cases (10), with triple-negative BC (TNBC) exhibiting the most substantial increase in expression of HKMTs (11). In BC, SETDB1 promotes MYC and cyclin D1 mRNA expression by augmenting internal ribosome entry site (IRES)-mediated translation. Simultaneously, the c-MYC-polycomb family transcriptional repressor axis reciprocally regulates SETDB1 expression, amplifying cellular proliferation and self-renewal capabilities (12). Acting as a ΔNp63α interactor, SETDB1 contributes to p63 protein stability, thereby promoting the self-renewal of BC stem cells (13). Additionally, SETDB1 induces epithelial-mesenchymal transition (EMT) and enhances migration and invasion by downregulating SMAD7 (9) and its effects can be reversed by microRNA (miRNA/miR)-7 (14) and -381-3p (15).

Given the association between protein localization and its physiological role in biological processes, determining localization of SETDB1 in cancer cells and the underlying mechanisms in metastasis is key. Both endogenous and exogenous SETDB1 have been identified in the cytoplasm (16). The nucleocytoplasmic trafficking of SETDB1 depends on chromosome region maintenance 1 (CRM1) protein, encompassing an N-terminal N255 region with a SUMO interaction motif site binding to promyelocytic leukemia nuclear body (17). Treatment with the CRM1 inhibitor, leptomycin B (LMB), obstructs SETDB1 export to the cytoplasm and combination with the proteosome inhibitor MG132 contributes to the accumulation of SETDB1 in the nuclear region (16). Wnt3a activation of canonical Wnt signaling induces cytoplasmic localization of SETDB1, whereas use of IWP2, a small molecule inhibitor of Wnt signaling, leads to the reduction of cytoplasmic SETDB1 expression (18). While SETDB1 is key for gene transcription, it also serves a role in catalyzing non-histone methylation in the context of cancer. SETDB1-mediated trimethylation of AKT on K64 residue enhances AKT ubiquitination by TNF receptor associated factor 6), promoting AKT membrane translocation and kinase activation (19). Elevated expression of SETDB1-mediated AKT K64 methylation is associated with poorer prognosis in patients with NSCLC (20). However, the function and mechanism of cytoplasmic SETDB1 in BC remain elusive.

The present study aimed to investigated the expression pattern of SETDB1 in both breast cancer samples and cell lines. We also examined the biological functions of cytoplasmic SETDB1 in breast cancer cells and explored the potential mechanisms of cytoplasmic SETDB1 involved in EMT and Warburg effect.

Materials and methods

Human tissue specimens and immunohistochemistry (IHC). All primary BC samples (n=172) along with normal breast epithelium tissue specimens at 50 mm adjacent to the corresponding cancer surgically resected in the first diagnosis and breast fibroadenoma tissue (n=50) were obtained from Affiliated Hospital of Jining Medical University (Jining, China, between August 2008 and August 2010. The average age of patients was 50.51±12.29 years. All subjects were female patients with Invasive Ductal Carcinoma (IDC) by breast biopsy or pathology, without chemotherapy or radiotherapy before operation. Male patients or non-IDC including invasive lobular carcinoma, inflammatory breast cancer and metaplastic breast cancer were excluded. The acquisition was conducted with informed consent from the patients, adhering to protocols approved by the Ethics Committee of Jining Medical University. IHC detection was performed on 4-μm-thick 4% formalin-fixed (24 h, room temperature) and paraffin-embedded tissue slices. Before staining, slides were deparaffinized with xylene and tissues were rehydrated with graded ethanol, then the slides were dried at 60˚C for 1 h. The slides were submerged in citrate repairing buffer (10 mmol/l, pH 6.0) in microwave at 90˚C for 30 min and allowed to cool to room temperature. After being soaked in methanol containing 3% hydrogen peroxide for 10 min, the sections were washed with 1X Tris Buffered Saline (TBS) three times, 5 min) and blocked with 10% goat serum (Beyotime Institute of Biotechnology; cat. no. #C0265) for 30 min at 37˚C. The slides were incubated with polyclonal rabbit anti-SETDB1 antibody (Proteintech Group, Inc.; cat. no. #11231-1-AP, dilution 1:100) overnight at 4˚C. IgG antibody was utilized as a negative control in BC tissues. SETDB1 staining in normal breast epithelium and breast fibroadenoma tissues was used as positive control. After incubation, the slides were washed with 1x TBS and incubated with ready-to-use secondary anti-rabbit biotinylated antibody (Vector Laboratories; cat. no. #BP-9100-50) at RT for 1 h. After washed again, the sections were treated with 3,3'-diaminobenzidine (ZSGB-BIO, #ZLI-9019). In addition, tissues were stained with hematoxylin at room temperature for 3 min, dehydrated, cleared and mounted with Distyrene Plasticizer Xylene (VMR International, LLC; cat. no. #100504-938). Micrographs were captured by a light microscope. The assessment of SETDB1 staining involved the independent evaluation by two experienced pathologists, assigning scores of 0, 1, 2 and 3, corresponding to negative, weak, medium and high expression, respectively. Intensity scores were determined based on the percentage of positively stained tumor cells (<10, 1; 11-50, 2; ≥51%, 3). The final score was calculated as follows: Staining score x intensity score. Patients were then categorized as having either low or high SETDB1 expression, determined by the cut-off score (nuclear SETDB1 expression: 2.53; cytoplasmic SETDB1 expression: 2.62).

Cell culture and drug treatment. All breast cancer cell lines including MCF7, T47D, BT549, MDA-MB-231 were obtained from the Type Culture Collection of Chinese Academy of Sciences (Shanghai, China) and cultured in DMEM (Gibco, #11965092) or RPMI-1640 medium (cat. no. #11875093) with 10% fetal bovine serum (FBS; all Gibco, #16140071). The cultures were maintained in a humidified incubator at 37˚C with 5% CO_2. LMB (Beyotime Institute of Biotechnology; cat. no. #S1726) or recombinant human Wnt3a protein (Proteintech, #HZ-1296) was introduced into the serum-free medium at 37˚C with a concentration of 200 nM or 50 ng/ml for 24 h, respectively, while 0.1% DMSO served as the control.

Lentiviral vector infections and small interfering (si)RNA transfection. The lentiviral SETDB1 overexpression and short hairpin RNA vectors were constructed and introduced into cell lines. A stably overexpressed (MCF7/SETDB1) and a stably depleted SETDB1 cell line (BT549/shSETDB1) were established as described in a previous study (21). The lactate dehydrogenase A (LDHA) overexpression plasmid was constructed by cloning the coding region of human LDHA into the pLVX-IRES-PURO-3xFlag vector generated by OBiO Technology (Shanghai) Corp., Ltd. For siRNA transfections, three siRNAs targeting the human LDHA gene, along with negative control (siCtrl), were procured from JianRan as follows: siLDHA#1 (5'-GCUGAUUUAUAAUCUUCUA-3'), siLDHA#2 (5'-GAAUAAGAUUACAGUUGUU-3') and siLDHA#3 (5'-GACUGAUAAAGAUAAGGAA-3'). A total of $1x10^5$ cells/well was seeded into six-well plate; 24 h later, the siRNAs were transfected into cells using Lipofectamine RNAiMAX (Invitrogen; Thermo Fisher Scientific, Inc.; cat. no. #13778) for 48 h at 37˚C.

Immunofluorescence staining. Cultured cells were fixed in 4% paraformaldehyde for 10 min at room temperature, followed by washing in PBS and permeabilization with 0.1% Triton X-100 for 30 min at RT. Subsequently, cells were blocked with 10% goat serum (Beyotime Institute of Biotechnology; cat. no. #C0265) for 1 h at RT and exposed to SETDB1 antibody (cat. no. #HPA018142; Sigma-Aldrich; Merck KGaA; 1:100) at 4˚C overnight, followed by Alexa Fluor 488-conjugated secondary antibody (Abcam, #ab150073, dilution: 1:200) for 1 h at room temperature. For visualizing the cytoskeleton, nuclear staining with Hoechst 33342 (Thermo Fisher Scientific, #62249, dilution: 1:200) at RT in the dark for 5 min was used, along with F-actin staining using phalloidin (Abcam, #ab176753; 1:1,000) for 1 h at RT. Images were captured using Axionvision software v4.8 (zeiss.com) and a Carl Zeiss fluorescence microscope (magnification, x200).

Subcellular fraction extraction and western blot analysis. Subcellular fractions of nuclei or cytoplasm were isolated by Minute™ Cytoplasmic and Nuclear Fractionation kit (Invent Biotechnologies, Inc.; cat. no. #SC-003) according to the manufacturers' protocol. The extracted proteins were examined via western blot using β-actin (Cell Signaling Technology, Inc. cat. no. #4970S) serving as marker for total and cytoplasmic protein, Lamin A antibody (CSignaling Technology, Inc.; cat. no. #86846S) serving as marker for nuclear protein. Western blot was performed as described in a previous study (21). Primary antibody against p53 (cat. no. #60283-2-Ig, 1:1,000), Kras (cat. no. #12063-1-AP, 1:1,000), pan-Ras (cat. no. #60309-1-Ig, 1:1,000), AKT (cat. no. #60203-2-Ig, 1:1,000), phosphorylated (p-)AKT (Ser473; cat. no. #80455-1-RR, 1:1,000), p-AKT (Thr308; cat. no. #29163-1-AP, 1:1,000), c-MYC (cat. no. #67447-1-Ig; 1:1,000), LDHA (cat. no. #21799-1-AP, 1:1,000) and GAPDH (cat. no. #60004-1-Ig, 1:2,000) were obtained from ProteinTech Group, Inc.; p-c-MYC (Ser293; cat. no. #PA5-105447, 1:2,000) was obtained from Invitrogen (Thermo Fisher Scientific, Inc.) and p-MYC (T58 + S62; cat. no. #13342, 1:1,000) was obtained from Signalway Antibody LLC. Antibodies against E-cadherin, N-cadherin, vimentin, Snail and Slug were obtained from EMT Antibody Sampler kit (cat. no. #9782; Cell Signaling Technology, Inc.; 1:1,000).

Reverse transcription-quantitative (RT-q)PCR analysis. Total RNA was extracted from cells with RNAiso plus obtained (Takara Biotechnology Co., Ltd.; cat. no. #9108) and its concentration was determined using a NanoDrop spectrophotometer. RNA was reverse-transcribed to cDNA using PrimeScript RT Master Mix (Takara Biotechnology Co., Ltd.; cat. no. #DRRO36A) according to the manufacturer's instructions. cDNA was amplified utilizing SYBR Premix Ex Taq (Takara Biotechnology, cat no. #RR420A) with specific primer pairs for the c-MYC, LDHA and β-actin genes. The primer pairs (Sangon Biotech Co., Ltd.) were as follows: MYC forward, 5'-CGACGAGACCTTCATCAAAAAC-3' and reverse, 5'-CTTCTCTGAGACGAGCTTGG-3'; LDHA forward, 5'-TCAGCCCGATTCCGTTACCTAATG-3' and reverse, 5'-CACCAGCAACATTCATTCCACTCC-3' and β-actin forward, 5'-CCCAGATCATGTTTGAGACC-3' and reverse, 5'-AGGGCATACCCCTCGTAGAT-3'. The thermocycle conditions consisted of one cycle at 95˚C for 10 min, followed by 40 cycles of amplification at 95˚C for 15 sec, and then 60˚C for 1 min. Following normalization to β-actin, the expression levels were quantified using 2-ΔΔCq method (22), with all experiments conducted in triplicate.

Wound healing assay. BT549, T47D and MCF7 cells were seeded in six-well plates reaching 70-80% confluence with 2 ml complete medium. Following cell adhesion, a scratch was introduced using a pipette tip and the dislodged cells were washed with PBS. BT549 cells were cultured in serum-free medium with DMSO or LMB treatment for 24 or 48 h. T47D and MCF7 cells were cultured in RPMI-1640 or DMEM with 10% FBS for 24 h or 48 h. Images of the scratched area were captured with a light microscope (magnification, x100) at 24 and 48 h. Accurate wound measurements were taken to calculate the wound closure=(wound width at 0 h-wound width at 24 or 48 h)/wound width at 0 h.

Migration and invasion assay. The migration assay used Transwell chambers (Corning, Inc.; cat. no. #3422); for the invasion assay, inserts were precoated with Matrigel (BD Biosciences; #354234) and at 37˚C for 4 h. In the upper chambers, a total of $5x10^4$ cells were seeded in 200 μl serum-free DMEM medium; in the lower chamber, 500 μl DMEM medium containing 10% FBS was added. Cells were incubated at 37˚C for 24 h, then fixed with methanol for 10 min at RT and stained with 0.1% crystal violet for 20 min at room temperature. Following PBS washes and air-drying, cells were photographed using a light microscope (magnification, x200) and counting was performed manually across five semi-random, non-overlapping areas and average value was calculated.

Metabolite detection. Detection of glucose, pyruvate, lactate production and ATP content in cells was performed using glucose dehydrogenase (cat. no. M011), pyruvate (cat. no. A081), lactate (cat. no. A019) and ATP assay kits (cat. no. A095; all Nanjing Jiancheng Bioengineering Institute) according to the manufacturer's instructions.

Transcriptome sequencing and bioinformatics analysis. RNA-seq was performed by BGI, Inc. Briefly, total RNA extraction was performed using TRIzol reagent (Thermo Fisher Scientific, #15596026) and Optimal Dual-mode mRNA Library Prep Kit (BGI, Inc.; #LR00R96) was used for constructing the mRNA library according to the manufacturer's instructions. mRNA was isolated using 50 μl magnetic beads (Beckman; cat. no. #A63880) with Oligo (dT) attached and fragmented using a Frag/Prime Buffer (BGI, Inc.; cat. no. #LR00R96-E). Subsequently, through random hexamer-primed RT), first-strand cDNA was generated (25˚C, 10 min; 42˚C, 15 min; 70˚C, 15 min; 4˚C, hold), followed by second-strand cDNA synthesis (16˚C, 30 min; 72˚C, 15 min; 4˚C, hold). Following repair incubation (20˚C, 15 min), A-Tailing Mix and RNA Index Adapters (BGI Plug-In Adapter Kit) were introduced. The cDNA underwent PCR amplification (1 cycle: 98˚C, 1 min; 16 cycles: 98˚C, 10 sec, 60˚C, 30 sec, 72˚C, 30 sec, 72˚C, 5 min; hold, 4˚C), purification using 50 μl Ampure XP Beads (Beckman, #A63880) at RT for 5 min and dissolution in 52 μl Elution Buffer (BGI, Inc.; #LR00R96-N)

at RT for 5 min. The double-stranded PCR products were denatured by heat and circularized using the splint oligo sequence (5'-GAACGACATGGCTACGATCCGACTTAAGTCGGAGGCCAAGCGGTCTTAGGAAGACAACAACTCCTTGGCTCTCACA-3'). The single-strand circle DNA was formatted as the final library and amplified with phi29 to create DNA nanoballs (DNBs). Using the BGIseq 500 platform (BGI, China), DNBs were fed into the patterned nanoarray, producing single-end 50 base reads. Bioinformatics analysis was conducted by BGI, China. Differentially expressed genes (DEGs) were identified using the limma package in R software v3.3.2 (https://www.r-project.org/), with a cutoff of |log2FC|>1 and FDR<0.05. Gene Ontology (GO; geneontology.org/) and Kyoto Encyclopedia of Genes and Genomes (KEGG; genome.jp/kegg/) pathway analysis was performed using the R software v3.3.2 module profiler package (https://cran.r-project.org/web/packages/profileR/index.html) with a criterion of P<0.05.

Immunoprecipitation (IP) and liquid chromatography-mass spectrometry (LC-MS). Cytoplasmic protein (100 μg/IP reaction) was extracted as aforementioned and incubated with SETDB1 antibody (2 ug per IP (Proteintech Group, Inc.; cat. no. 11231-1-AP) and 30 μl Protein G agarose beads (cat. no. #37478; Cell Signaling Technology, Inc.) by rocking at 4˚C overnight. The beads were washed with 1 ml Nonidet P-40 (Thermo Fisher Scientific, Inc.; cat. no. #85124) buffer three times and resuspended in 2X SDS loading buffer. Subsequently, LC-MS was performed by APPLIED PROTEIN TECHNOLOGY, Inc (Shanghai Zhongkexin Life Biotechnology Co., Ltd.). Briefly, proteins were integrated into buffer (4% SDS, 100 mM DTT, 100 mM Tris) and digested with trypsin and the resulting peptides were collected as a filtrate. DTT (Sigma-Aldrich; Merck KGaA; cat. no. #3483-12-3) and indole-3-acetic acid (IAA) (Sigma-Aldrich, #87-51-4) were added to alkylate proteins. Protein digestion was performed using trypsin and halted by trifluoracetic acid. Gel pieces were excised from SDS-PAGE and subjected to three extractions with 60.0% Acetonitrile (Sigma-Aldrich, #76-05-8)/0.1% Trifluoroacetic Acid (both Sigma-Aldrich, #76-05-1). Each fraction was injected for nano LC with tandem mass spectrometry (LC-MS/MS) analysis. The resulting peptides were analyzed using Thermo Fisher Orbitrap Elite with Waters NanoAcuity Ultra-Performance LC) (Thermo Fisher Scientific, Inc.). MS/MS data were searched against the Uniprot Human protein database (uniprot.org/) using Mascot 2.5.1 (https://www.matrixscience.com/) and data analysis was performed using Scaffold 4.4.8 software (https://researchexperts.utmb.edu/en/equipments/scaffold-version-448-informatics-software). Peptides and modified peptides were accepted if they passed 1% FDR threshold.

Statistical analysis. Statistical analysis was conducted utilizing IBM SPSS Statistics 20 (ibm.com/products/spss-statistics) or GraphPad Prism 10 software (https://www.graphpad.com/). Data from triplicate tests are presented as the mean ± SD. χ^2 or Fisher's exact test was used to compare clinicopathological features between SETDB1 high and low groups. Correlations were estimated by Spearman's correlation. Two-tailed unpaired Student's t test and one-way ANOVA with Tukey's post hoc test were used to determine the statistical significance of differences between groups. P<0.05 was considered to indicate a statistically significant difference.

Results

Cytoplasmic expression of SETDB1 is positively associated with lymph node metastasis and more aggressive subtypes in patients with BC. To assess the SETDB1 expression, IHC was performed on paraffin-embedded BC samples. SETDB1 was expressed in both the nucleus and cytoplasm of BC tissues, whereas only nuclear staining was observed in breast fibroadenoma tissue. SETDB1 was not expressed in normal breast epithelium cells (Fig. S1). Based on staining score, patients were categorized into SETDB1 high or low expression groups. No significant differences were observed between nuclear staining of SETDB1 and clinicopathological factors, including age, tumor size, TNM stage, lymph node metastasis, progression and survival (Table I). However, a positive correlation was identified between cytoplasmic SETDB1 and lymph node metastasis (Table II). Furthermore, high cytoplasmic SETDB1 was more prevalent in patients with high HER2 expression (42.86%) and TNBC subtypes (43.90%) compared with luminal subtype (28.18%; Table III). Taken together, these findings indicate that cytoplasmic SETDB1 is associated with more aggressive BC subtypes and metastasis.

Localization of endogenous and exogenous SETDB1 protein in BC cells. To confirm SETDB1 localization, immunofluorescence was performed in MCF7 and BT549 cells. Endogenous SETDB1 was predominantly expressed in the nucleus in MCF7 cells with punctuate signals, while both nuclear and cytoplasmic signals in a diffuse pattern were observed in BT549 cells (Fig. 1A). Subcellular distribution of endogenous SETDB1 was evaluated by separately extracting nuclear and cytoplasmic fractions and immunoblotting. Although the total protein expression of SETDB1 was higher in MCF7 and T47D compared with BT549 and MDA-MB-231 cells, its localization was predominantly nuclear rather than cytoplasmic (Fig. 1B). Conversely, endogenous SETDB1 was primarily detected in the cytoplasm of BT549 and MDA-MB-231. To determine subcellular localization of exogenous SETDB1, a stably overexpressed SETDB1 cell line (MCF7/SETDB1) was established as described in a previous study (21). Exogenous SETDB1 was primarily found in the cytoplasm, with only a few signals detected in the nucleus (Fig. 1C). Taken together, these findings suggested a potential association between distribution of SETDB1 protein and its function in BC, indicating a potential mechanism underlying SETDB1 transport from the nucleus to the cytoplasm.

LMB blocks, while Wnt3a induces SETDB1 transport from nucleus to cytoplasm. SETDB1 encompassing nuclear localization signals (NLSs) and nuclear export signals (NESs) which indicate that SETDB1 is able to shuttle between the cytoplasm and nucleus (16). CRM1 protein facilitates transportation of SETDB1 from the nucleus to the cytoplasm (16). To validate the impact of CRM1 on SETDB1 transportation, LMB was used to bind CRM1 and inhibit

Table I. Correlation between nuclear SETDB1 expression and clinicopathological factors.

Factor	All (n=172)	SETDB1 expression		r	P-value
		Low (n=86)	High (n=86)		
Age, years				-0.062	0.418
≤35	18	8	10		
36-51	77	37	40		
>51	77	41	36		
Tumor size, cm				-0.005	0.990
<2	96	48	48		
2-5	69	34	35		
>5	7	4	3		
TNM stage				-0.003	0.966
I	62	32	30		
II	77	36	41		
III-IV	33	18	15		
Number of LN metastases				0.036	0.635
0	100	50	50		
1-3	42	24	18		
4-9	20	10	10		
>9	10	2	8		
Tumor progression				-0.173	0.261
Absent	55	27	28		
Present	8	6	2		
Death				-0.02	0.877
No	52	27	25		
Yes	11	6	5		

SETDB1, SET domain bifurcated 1; LN, lymph node.

its activity in BT549 cells. Following 8 h treatment with LMB, SETDB1 was predominantly detected in the nucleus (Fig. 2A). In comparison, with DMSO as a control, SETDB1 was found in both the nucleus and cytoplasm, confirming that CRM1-mediated SETDB1 shuttling between the nucleus and cytoplasm was inhibited by LMB. Cytoplasmic SETDB1 expression depends on canonical Wnt signaling during myoblast differentiation (18). Recombinant Wnt3a protein was used to activate Wnt signaling. Following 24 h Wnt3a treatment in MCF7 cells, increased cytoplasmic localization of SETDB1 was observed compared with the control group (Fig. 2B). These results suggested a mechanism that regulates SETDB1 transportation between nucleus and cytoplasm, involving the interplay of CRM1 and Wnt signaling pathways.

CRM1 inhibitor decreases migration and invasion and reverses SETDB1-induced EMT. To investigate the impact of SETDB1 shuttling from the nucleus to the cytoplasm on migration and invasion abilities of BC, wound healing and Transwell assays were performed following treatment with LMB or DMSO. The wound healing rate in BT549 cells was significantly lower following LMB treatment at both 24 and 48 h compared with the control group (Fig. 3A). Similarly, Transwell assay revealed that LMB significantly reduced migration and invasion abilities in BT549 (Fig. 3B) as well as MCF7/SETDB1 cells (Fig. 3C). Morphological change was observed in MCF7/SETDB1 cells following LMB treatment for 36 h from long spindle forms to polygonal shapes (Fig. 3D). Furthermore, immunoblotting showed that mesenchymal marker vimentin expression decreased, while epithelial marker E-cadherin expression increased in MCF7/SETDB1 + LMB cells (Fig. 3E), indicating that LMB treatment reversed SETDB1-induced EMT by inhibiting cytoplasmic SETDB1. In summary, cytoplasmic SETDB1 served critical roles in migration, metastasis and EMT.

Cytoplasmic SETDB1 enhances the Warburg effect and LMB treatment reverses SETDB1-induced Warburg effect. To determine the molecular mechanism underlying involvement of cytoplasmic SETDB1 in BC cells, total RNA was extracted from MCF7/NC + DMSO, MCF7/SETDB1 + DMSO and MCF7/SETDB1 + LMB cells. RNA-sequencing analysis revealed 1,575 up- and 2,132 downregulated genes in the MCF7/SETDB1 + LMB group compared with the MCF7/SETDB1 + DMSO group (Fig. 4A). KEGG analysis demonstrated that DEGs were enriched in various metabolism pathways, such as 'glutathione

Table II. Correlation between cytoplasmic SETDB1 expression and clinicopathological factors.

		SETDB1 C expression			
Factor	All (n=172)	Low (n=114)	High (n=58)	r	P-value
Age, years				-0.032	0.673
≤35	18	11	7		
36-51	77	51	26		
>51	77	52	25		
Tumor size, cm				-0.100	0.197
<2	96	60	36		
2-5	69	48	21		
>5	7	6	1		
TNM stage				-0.133	0.082
I	62	38	24		
II	77	49	28		
III-IV	33	27	6		
Number of LN metastases				0.167	0.029[a]
0	100	72	28		
1-3	42	27	15		
4-9	20	11	9		
>9	10	4	6		
Tumor progression				-0.223	0.102
Absent	55	39	16		
Present	8	8	0		
Death				0.020	1.000
No	52	39	13		
Yes	11	8	3		

[a]P<0.05. SETDB1, SET domain bifurcated 1; LN, lymph node.

Table III. Correlation between cytoplasmic SETDB1 expression and breast cancer subtype.

		SETDB1 expression			
Subtype	Total	Low (%)	High (%)	r	P-value
Luminal	110	79 (71.82)	31 (28.18)	0.154	0.044[a]
HER2	21	12 (57.14)	9 (42.86)		
Triple negative	41	23 (56.10)	18 (43.90)		

[a]P<0.05.

metabolism', 'butanoate metabolism' and 'pentose and glucuronate interconversions' (Fig. 4B). Additionally, GO analysis revealed enrichment in immune-related pathways, including 'adaptive immune response', 'immune response to tumor cell' and 'positive regulation of immune system process' (Fig. 4C). Reprogrammed metabolism, a hallmark of cancer, involves aerobic glycolysis, commonly known as the Warburg effect (23). To assess potential involvement of SETDB1 in the Warburg effect, levels of metabolic indicators, including glucose, pyruvate, lactate and ATP, were measured. Knockdown of SETDB1 in BT549 cells led to a significant decrease in the levels of these metabolites compared with the control group (Fig. 4D). Furthermore, in the absence of LMB, overexpressed SETDB1 increased levels of glucose, pyruvate, lactate and ATP in MCF7 cells. However, the metabolite levels decreased in the presence of LMB (Fig. 4E). These findings suggested that exogenous SETDB1 may enhance the Warburg effect by localizing to the cytoplasm and its impact was mitigated by inhibiting cytoplasmic SETDB1 with LMB.

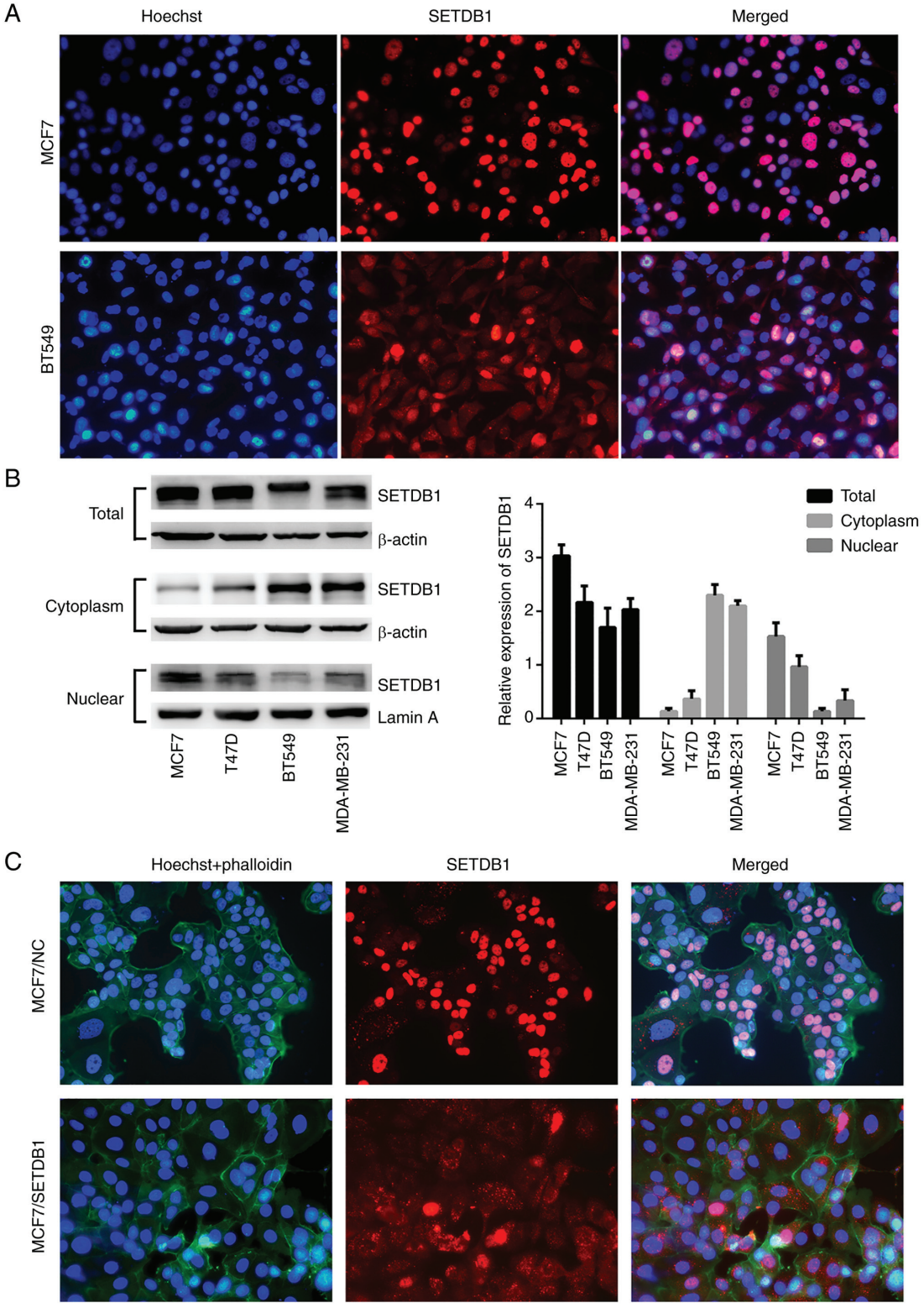

Figure 1. Localization of endogenous and exogenous SETDB1 in breast cancer cells. (A) Representative immunofluorescence of endogenous SETDB1 (red) localization in MCF7 and BT549 cells. (B) Immunoblotting analysis of endogenous SETDB1 in total nuclear and cytoplasmic fractions of breast cancer cell lines. (C) Representative immunofluorescence of exogenous SETDB1 (red) localization in MCF7 cells. Nuclei are stained with Hoechst (blue) and the cytoskeleton is visualized with phalloidin (green). Magnification, x200. SETDB1, SET domain bifurcated 1.

Cytoplasmic SETDB1 upregulates c-MYC/LDHA signaling and activates its downstream signaling pathway. Numerous studies (24,25) have demonstrated the key role of diverse pathways in the Warburg effect, including the PI3K/AKT/mTOR, hypoxia-inducible factor-1 (HIF-1), Kras, p53 and MYC pathways. Therefore, cytoplasmic protein isolation and immunoblotting analysis were conducted in MCF7/SETDB1 cells in the presence or absence of LMB. Decreased in p53 expression and an increase in Kras, pan-Ras, AKT and p-AKT (Ser473) were noted in SETDB1-overexpressing

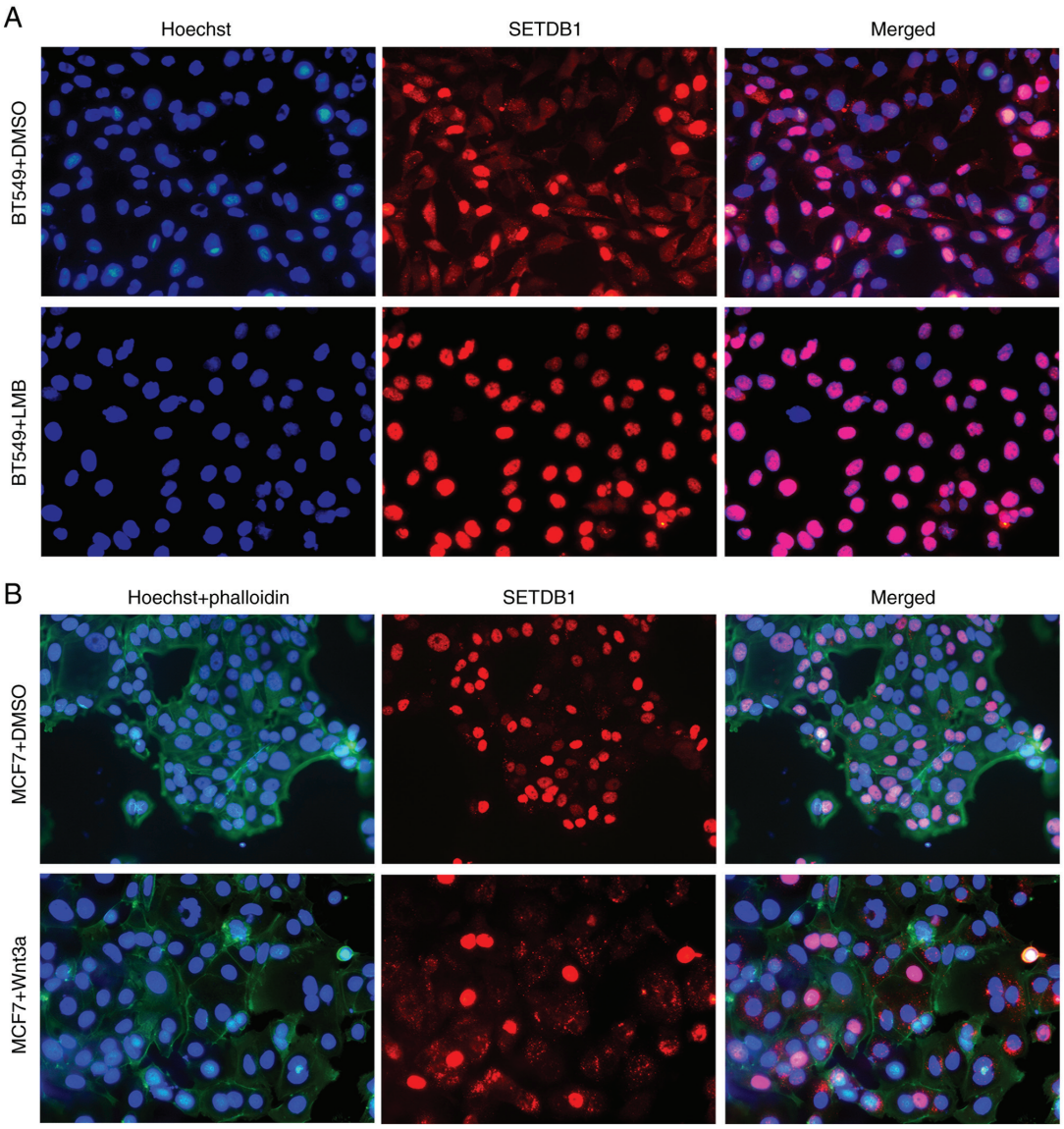

Figure 2. Regulation of SETDB1 transportation from nucleus to cytoplasm. Representative immunofluorescence showing SETDB1 (red) detection following (A) LMB treatment in BT549 cells and (B) Representative recombinant Wnt3a protein treatment in MCF7 cells. DMSO was used as the control group. Nuclei are stained with Hoechst (blue) and cytoskeleton is visualized with phalloidin (green). Magnification, x200. SETDB1, SET domain bifurcated 1.

cells. However, no significant changes were found between the MCF7/SETDB1 + DMSO and MCF7/SETDB1 + LMB groups (Fig. 5A). Conversely, cytoplasmic expression of c-MYC and its phosphorylated proteins significantly increased in MCF7/SETDB1 + DMSO cells; this effect was attenuated after LMB treatment (Fig. 5B). Consistently, RT-qPCR results demonstrated elevated c-MYC mRNA expression in SETDB1-overexpressing cells, which was decreased following LMB treatment (Fig. 5C). These data revealed that cytoplasmic SETDB1 upregulated c-MYC expression and activated its downstream signaling pathway. LDHA, a key enzyme in the Warburg effect, is known to be controlled by c-MYC (26). Consequently, the cytoplasmic content of LDHA was examined through immunoblotting, revealing increased LDHA expression in MCF7/SETDB1 cells and decreased levels of LDHA in cells treated with LMB (Fig. 5D). In summary, these results suggested that cytoplasmic SETDB1 upregulated the c-MYC/LDHA pathway and inhibition of cytoplasmic SETDB1 abolished this effect.

LDHA overexpression promotes migration and invasion and induces EMT in BC cells. SETDB1, functioning as a histone lysine methyltransferase, has been reported to mediate lysine methylation of non-histone proteins in various types of cancer, such as non-small cell lung cancer (19,20,27). To investigate methylation of cytoplasmic proteins catalyzed by SETDB1, IP and LC-MS analysis were performed to identify methylated residues binding with SETDB1 (Fig. S2A). A total of 5,826 peptides were detected and 513 methylated residues were identified. GO analysis revealed enrichment in cellular process, metabolic process, localization and immune system process for these proteins (Fig. S2B). Notably, the di-methylation of LDHA at lysine 155 (K155) was identified (Fig. S2C). Furthermore, IP confirmed the binding of LDHA and SETDB1 (Fig. S3). To determine the function of LDHA in BC cells, a stably expressed T47D/LDHA cell line was established and the infection efficiency was verified by immunoblotting and RT-qPCR (Fig. 6A). Due to the Flag tag in the vector, two bands of LDHA were evident in overexpressing cells, with the

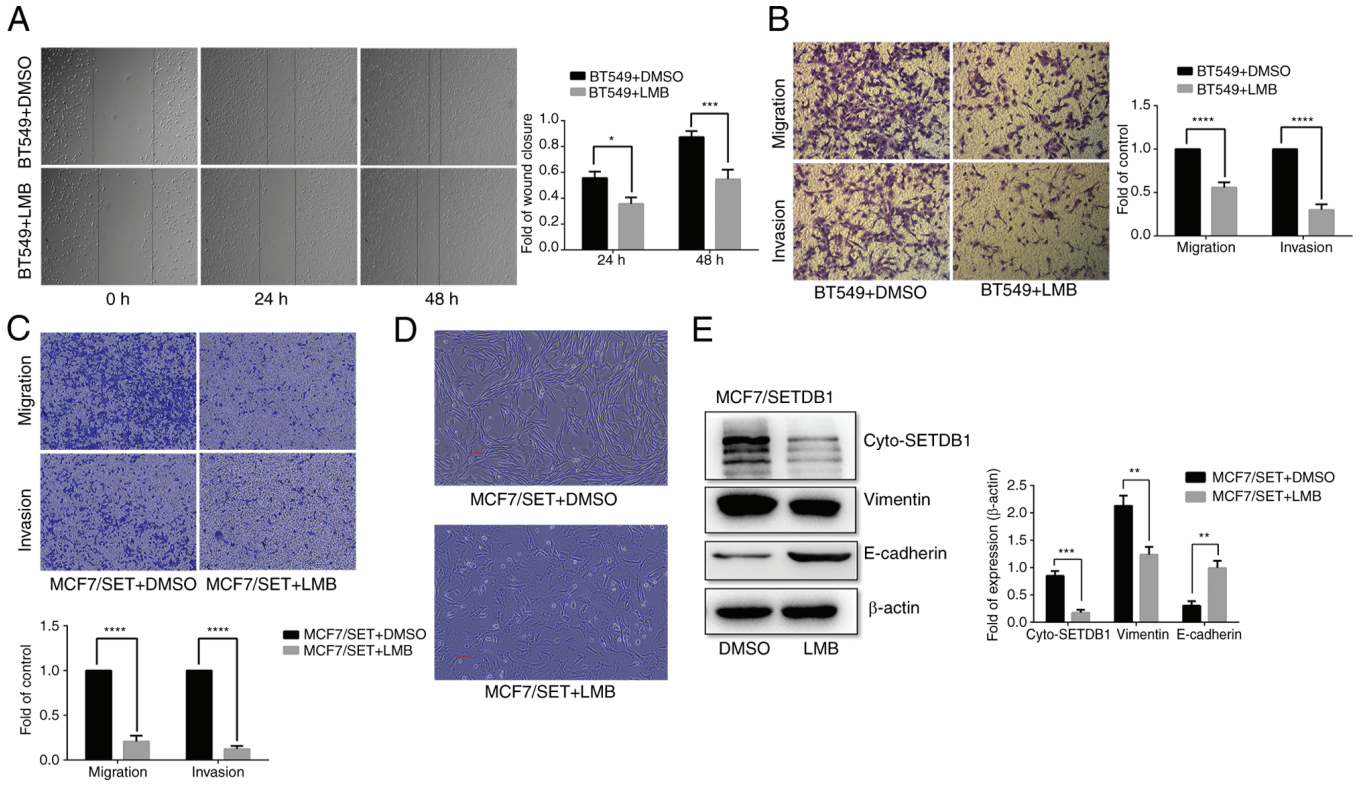

Figure 3. Cyto-SETDB1 enhances migration and invasion and induces epithelial-mesenchymal transition *in vitro*. (A) Wound healing and (B) Transwell assay in BT549 cells following LMB or DMSO treatment. Magnification, x100. (C) Transwell assay in MCF7/SETDB1 cells following LMB treatment. DMSO is used as the control group. Magnification, x200. (D) Morphology changes of MCF7/SETDB1 cells following LMB treatment. (E) Expression of cyto-SETDB1, vimentin and E-cadherin in MCF7/SETDB1 cells. *P<0.05, **P<0.01, ***P<0.001, ****P<0.0001. Cyto-SETDB1, cytoplasmic SET domain bifurcated 1; LMB, leptomycin B.

red band representing exogenously expressed LDHA and the black band indicating endogenously expressed LDHA. Wound healing and Transwell assay revealed that LDHA overexpression significantly promoted migration and invasion in T47D cells compared with the control (Fig. 6B and C). T47D/LDHA cells exhibited distinct morphological changes, displaying a spindle-shaped morphology (Fig. 6D). Furthermore, immunoblotting demonstrated that epithelial marker E-cadherin was decreased, while mesenchymal makers N-cadherin and vimentin, as well as EMT-associated transcription factors Snail and Slug, were increased in LDHA-overexpressing T47D cells (Fig. 6E). Collectively, these data demonstrated that LDHA enhanced migration and invasion by inducing EMT in BC cells.

Knockdown of LDHA decreases SETDB1-induced EMT and Warburg effect in BC cells. To assess the crucial role of LDHA in the function of SETDB1 in BC cells, LDHA was knocked down in SETDB1-overexpressing MCF7 cells. Following the confirmation of LDHA expression via immunoblotting and RT-qPCR (Fig. 7A), siLDHA2# and siLDHA3# showed significant decreases in both mRNA and protein level of LDHA and thus were chosen for subsequent investigation. LDHA knockdown significantly decreased migration and invasion abilities in SETDB1-overexpressing cells (Fig. 7B). Compared with control cells, wound healing assay demonstrated a significant decrease in cell migration following LDHA depletion (Fig. 7C). Additionally, levels of glucose, pyruvate, lactate and ATP were significantly decreased in LDHA knockdown cells (Fig. 7D). Notably, LDHA knockdown led to an increase in the epithelial marker E-cadherin, while expression of mesenchymal markers N-cadherin and vimentin, as well as Snail and Slug, were decreased (Fig. 7E). In summary, these findings demonstrated the essential role of LDHA in SETDB1-induced EMT and Warburg effect in BC cells.

Discussion

HKMTs constitute a group of enzymes that regulate transcription, chromatin architecture and cellular differentiation by catalyzing site-specify methylation of lysine residues on histone proteins (28). Alterations, genetic translocation and modified gene expression associated with these HKMTs are frequently observed in cancer (29). Additionally, subcellular localization of several histone-modifying enzymes is known to regulate their functions. Enhancer of zeste Homolog 2 (EZH2) is primarily localized to the nucleus. However, there is evidence to suggest that EZH2 can also shuttle between the nucleus and cytoplasm and its subcellular localization may influence its activity and function (30). Although SETDB1 is exported from the nucleus to the cytoplasm (17), its role and regulation of cytoplasmic localization in BC are not yet fully understood. Here, IHC confirmed expression of SETDB1 protein in both the nucleus and cytoplasm in BC samples. Only cytoplasmic SETDB1 expression was correlated with lymph node metastasis and aggressive BC subtypes. Furthermore,

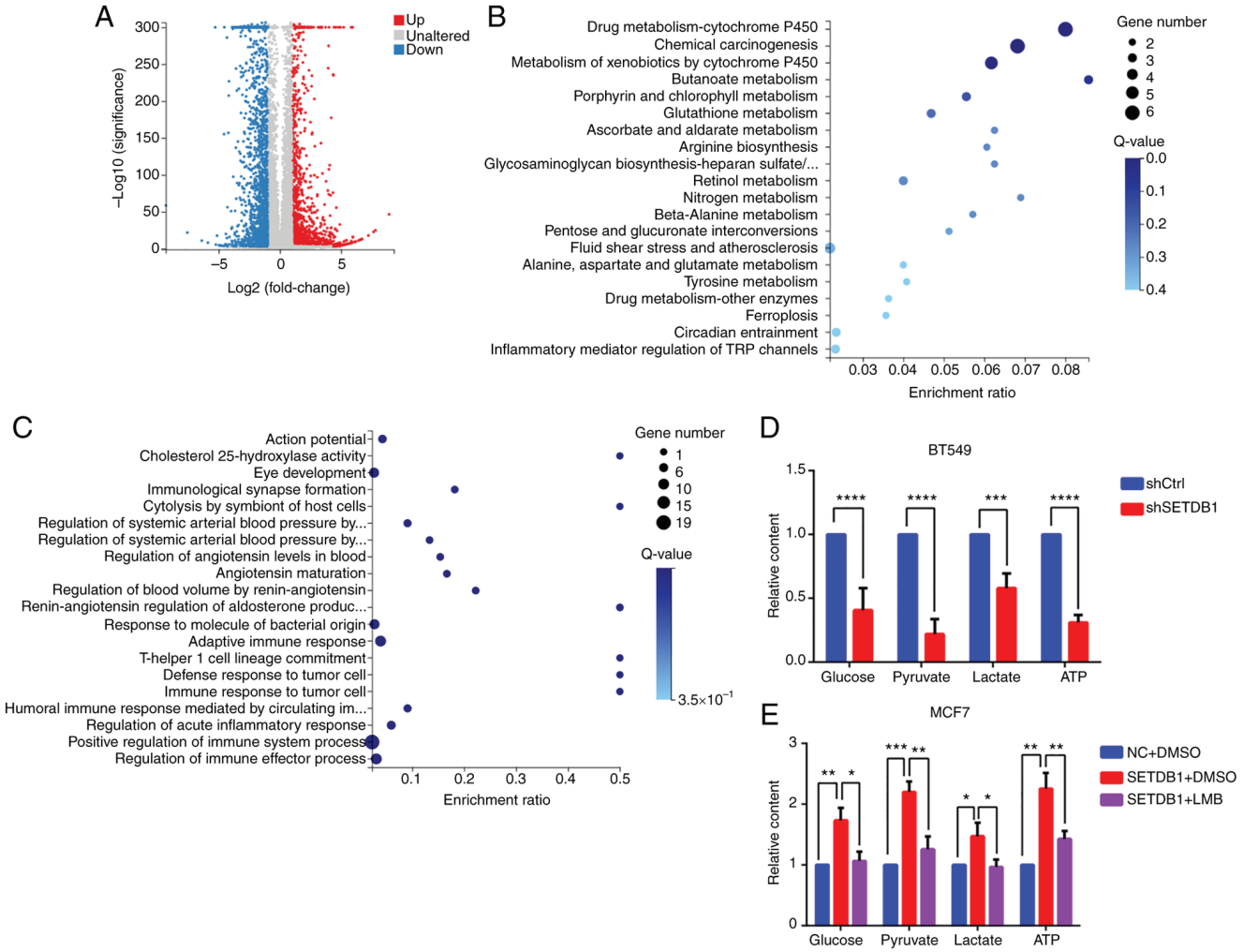

Figure 4. Cytoplasmic SETDB1 enhances the Warburg effect in breast cancer. (A) Volcano plot displaying DEGs in MCF7/SETDB1 cells with LMB or DMSO treatment. (B) Kyoto Encyclopedia of Genes and Genomes and (C) Gene Ontology pathways enrichment analysis of DEGs. (D) Metabolite levels in SETDB1-deficient BT549 and (E) in SETDB1-overexpressing MCF7 cells following LMB treatment. *P<0.05, **P<0.01, ***P<0.001, ****P<0.0001. SETDB1, SET domain bifurcated 1; LMB, leptomycin B; DEGs, differentially expressed genes; shCtrl, short hairpin RNA control; NC, negative control.

SETDB1 was predominantly expressed in the nucleus in MCF7 and T47D cells with limited migration and invasion ability. SETDB1 expression was mostly cytoplasmic in BT549 and MDA-MB-231 cells which are known of triple-negative breast cancer cell lines and characterized by strong migration and invasion ability (31).

The N-terminal region containing NES and NLS is responsible for cytoplasmic SETDB1 localization (17). Moreover, SETDB1 may undergo degradation by the proteosome and be exported to cytosol, mediated by CRM1 protein. Thus, combined treatment with LMB and MG132 contributes to the accumulation of SETDB1 in the nucleus (16). Conversely, Wnt3a treatment involving the Wnt/β-catenin pathway induces SETDB1 export to the cytoplasm (17). Tsusaka *et al* (32) reported that activating Transcription Factor 7-Interacting Protein 1, a known binding partner of SETDB1, antagonizes the nuclear localization of SETDB1 by binding to its N-terminal region and subsequently increases its ubiquitination. Consistent with these findings, the present study confirmed that LMB treatment inhibited SETDB1 export to the cytoplasm, and Wnt3a treatment contributed to the accumulation of cytoplasmic SETDB1.

To determine the function of cytoplasmic SETDB1 in BC migration and migration, *in vitro* experiments were performed in the presence or absence of CRM1 inhibitor treatment. A significant decrease in migration and invasion abilities was observed in BC cells with LMB treatment. Mechanistically, cytoplasmic SETDB1 was involved in various metabolism and immune-related pathways, such as 'pentose and glucuronate interconversions', 'immune response to tumor cell'. It has been reported that SUMOylated SETDB1 suppresses expression of lipid metabolism-associated target genes and downregulates lipid storage in adipocytes (33). SETDB1 also serves a crucial role in inhibiting endogenous retroviruses in primordial germ cells (34) and exogenous retroviruses in committed B lineage cells. Its loss also results in B lymphocyte failure and molecular abnormality (35). Moreover, loss of SETDB1 in pro-B cells leads to suppression of retrotransposon sequences such as endogenous murine leukemia virus and blocks B cell development (36). Studies have demonstrated the importance of SETDB1 in T cell development, partly due to suppression of Fc receptor IIB for IgG) (37,38). However, whether cytoplasmic SETDB1 is involved in metabolic reprogramming in BC remain unknown.

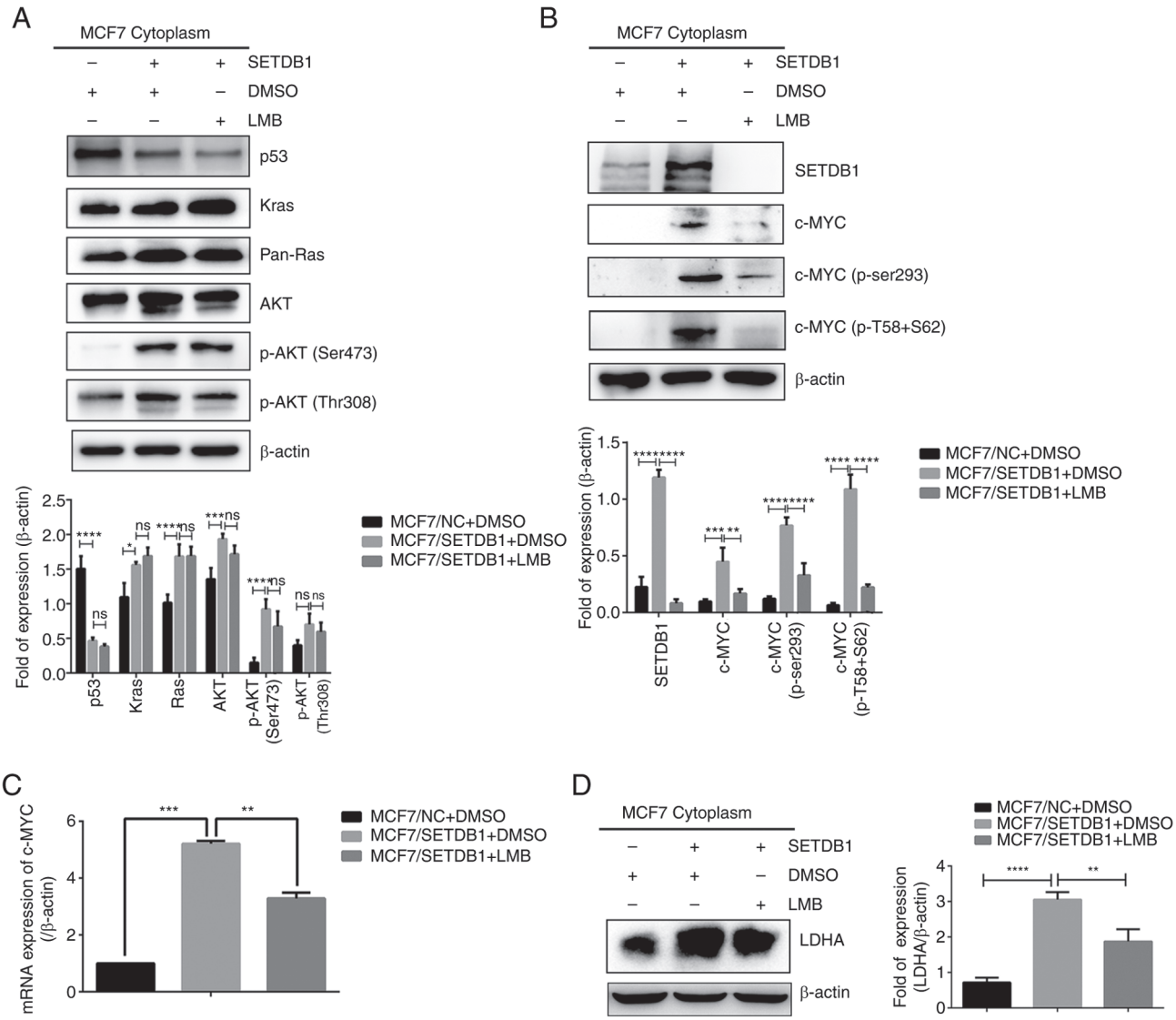

Figure 5. Cytoplasmic SETDB1 upregulates c-MYC/LDHA signaling pathway. (A) Cytoplasmic protein levels of p53, Kras, pan-Ras, AKT, p-AKT (Ser473) and p-AKT (Thr308) as well as (B) SETDB1, c-MYC, p-c-MYC (Ser293) and p-c-MYC (T58 + S62). (C) mRNA expression of c-MYC and (D) cytoplasmic protein expression of LDHA in MCF7/SETDB1 cells following LMB treatment. *P<0.05, **P<0.01, ***P<0.001, ****P<0.0001. SETDB1, SET domain bifurcated 1; LMB, leptomycin B; LDHA, lactate dehydrogenase A; pan-, pan-reactive; p-, phosphorylated.

Altered tumor metabolism has gained widespread acceptance as a hallmark of cancer (23) and enhances cell migration in most types of cancer (39). The Warburg effect, also known as aerobic glycolysis, occurs when cancer cells utilize glucose at an abnormally high rate in the presence of oxygen (40). More aggressive mesenchymal BC cell lines such as BT549 and MDA-MB-231 exhibit a greater Warburg effect with high rate of glycolytic to oxidative ATP flux compared with less aggressive epithelial lines such as MCF7 and T47D (39). To investigate whether SETDB1 regulates the Warburg effect, metabolite levels were detected. The results of metabolite detection showed that SETDB1-deficient cells exhibited a lower Warburg effect than controls. However, SETDB1 overexpression increased the contents of metabolite, which could be reversed by LMB treatment. To the best of our knowledge, the present study is the first to demonstrate the function of cytoplasmic SETDB1 in the Warburg effect. However, little is known about the underlying pathway by which SETDB1 affects the Warburg effect.

Several key signaling pathways involved in the Warburg effect, including PI3K/AKT/mTOR, Ras/Myc, reactive oxygen species/HIF-1, p53, and Kras (24). AKT binds to the Tudor domain of SETDB1, which binds demethylated lysine of H4-K20 and is involved in DNA repair (41). SETDB1 coordinates with AKT to suppress FOXO1 by enhancing AKT activation, while SETDB1 deficiency contributes to an increase in PTEN expression and induces apoptosis in spermatogonial stem cells (42). In paclitaxel-treated lung cancer cells, P53 works with histone lysine N-methyltransferase suppressor of Variegation 3-9 Homolog 1 to enhance H3K9me3 occupancy and inhibit SETDB1 transcription by directly binding to its promoter (43). Moreover, upregulation of SETDB1 suppresses apoptosis induced by 5-fluorouracil treatment in colorectal cancer cells by binding to the TP53 promoter region and inhibiting TP53 transcription (44). There is a positive regulation between SETDB1 and c-MYC in BC cells: SETDB1 increases c-MYC expression by IRES-mediated translation and c-MYC protein enhances SETDB1 expression by binding

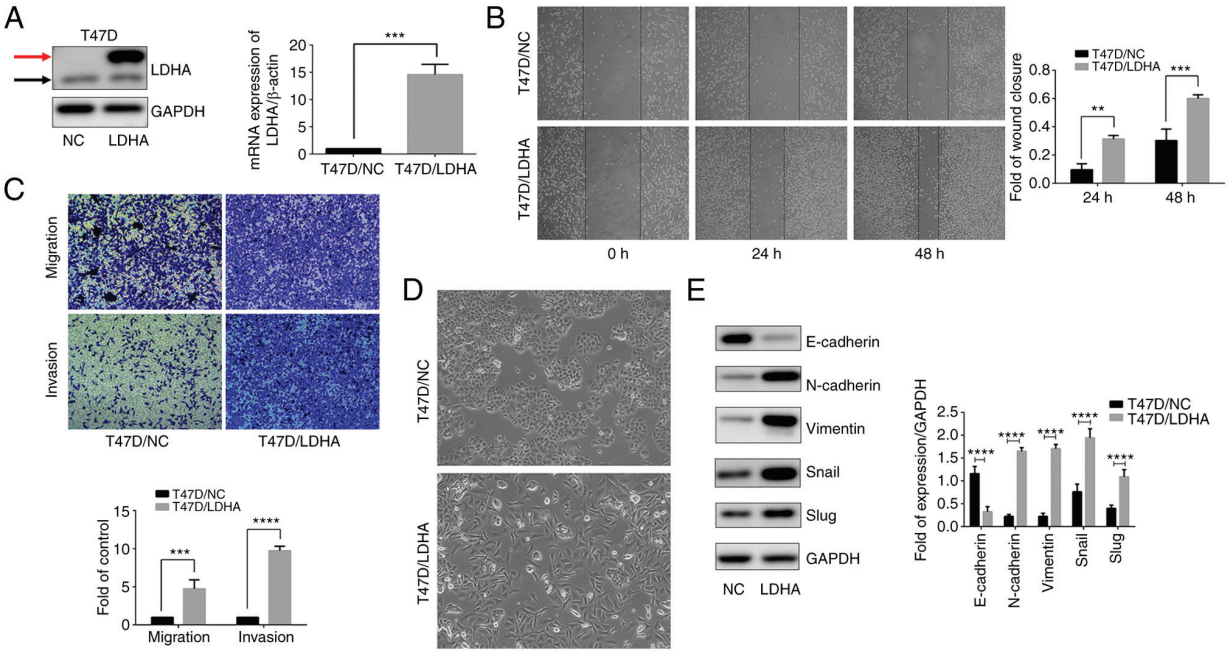

Figure 6. LDHA promotes migration and invasion and induces epithelial-mesenchymal transition in T47D cells. (A) Verification of LDHA expression in T47D cells by immunoblotting and reverse transcription-quantitative PCR. Red arrow: exogenous LDHA; black arrow: endogenous LDHA. (B) Wound healing (Magnification, x100) and (C) Transwell assay (Magnification, x200) detected migration and invasion in T47D/LDHA cells. (D) Morphology of LDHA-overexpressing T47D cells. Magnification, x200. (E) Protein levels of E-cadherin, N-cadherin, vimentin, Snail and Slug in T47D/LDHA cells. **P<0.01, ***P<0.001, ****P<0.0001. LDHA, lactate dehydrogenase A; NC, negative control.

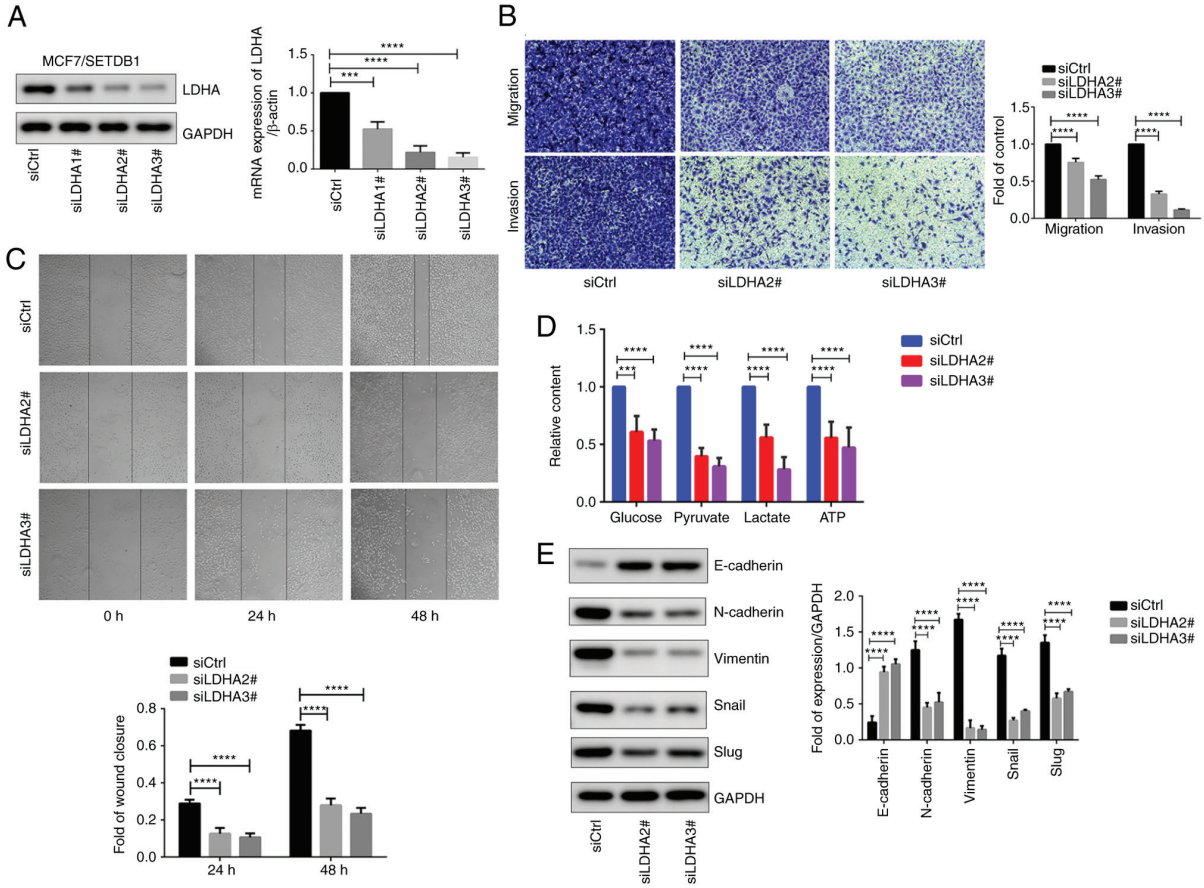

Figure 7. LDHA is key for SETDB1-induced migration, invasion, EMT and Warburg effect. (A) Detection of LDHA expression with immunoblotting and reverse transcription-quantitative PCR after transfecting three LDHA siRNAs in MCF7/SETDB1 cells. (B) Transwell assay. Magnification, x200. (C) Wound healing, Magnification, x100. (D) Metabolite levels in MCF7/SETDB1 cells following knockdown of LDHA. (E) Expression of EMT-associated genes and transcription factors in LDHA-deficient MCF7/SETDB1 cells. ***P<0.001, ****P<0.0001. LDHA, lactate dehydrogenase A; SETDB1, SET domain bifurcated 1; EMT, epithelial-mesenchymal transition; siCtrl, short hairpin RNA control.

to its promoter (12). Consistent with a previous study (24), the present study demonstrated that overexpression of cytoplasmic SETDB1 increased Kras, Ras, AKT and c-MYC expression. Furthermore, in the presence of LMB, decreased expression of c-MYC and its phosphorylated protein, as well as c-MYC-targeted gene LDHA in MCF7/SETDB1 cells, was observed. LDHA is known as an enzyme that catalyzes the final step of the Warburg effect by converting pyruvate to lactate (45). LDHA promotes migration and invasion of cancer cells by inducing EMT (46,47). Consistently, the present study confirmed that LDHA overexpression enhanced migration and invasion in BC cells and regulated EMT-associated genes and transcription factors. Therefore, the present study investigated how SETDB1 regulates (24) LDHA and whether LDHA is key for SETDB1-induced EMT and Warburg effect.

KMTs methylate non-histone proteins and certain SET domain-containing proteins are known to exclusively target non-histone substrates (48). SETDB1 is key for the methylation of the viral protein Tat at lysine residues 50 and 51 to inhibit the transcription of human immunodeficiency virus-1 long terminal repeat (49). In hepatocellular carcinoma, SETDB1 catalyzes di-methylation of p53 at 370 lysine residues, which decreases p53 protein stability by murine double minute 2-mediated ubiquitination (50). SETDB1 has been reported to interact with the Pleckstrin Homology domain of AKT and mediate methylation of AKT K140 to promote cell growth and glycolysis and drug resistance in a carcinogen-induced skin cancer model (19). Furthermore, SETDB1-mediated AKT K64 methylation is linked to carcinogenesis and a poor prognosis in patients with NSCLC (20). Here, LDHA bound to SETDB1 and dimethylation of LDHA at K155 was observed, suggesting that LDHA may be a novel non-histone substrate of SETDB1. Moreover, LDHA depletion reversed SETDB1-induced EMT and metabolic reprogramming.

There are several limitations in the present study. Firstly, the role of di-methylation of LDHA, catalyzed by SETDB1, in the induction of EMT remains unclear. Secondly, while inhibition of migration and invasion in gastric carcinoma cells by LMB treatment has been reported (51), the precise molecular mechanism underlying this phenomenon remains elusive. The present study suggested that SETDB1 may be a target gene of CMR1 inhibitor; however, further investigation is required to determine the impact of LMB on BC cells. Thirdly, a distant metastasis nude mouse model is required to confirm *in vivo* efficacy of CMR1 inhibitor on SETDB1-induced metastasis.

In conclusion, the present study demonstrated that cytoplasmic SETDB1 was associated with BC metastasis and the function of cytoplasmic SETDB1 in migration, EMT and metabolic reprogramming was blocked by a CMR1 inhibitor. Mechanically, cytoplasmic SETDB1 positively regulated the c-MYC/LDHA pathway and enhanced snail family transcriptional repressors. SETDB1 may be a potential target for individuals with MBC. Additionally, medications that aim at different regions, such as the NES/NLS regions responsible for SETDB1 nucleocytoplasmic shuttling, may offer therapeutic options (52). The present study provided insight into the function and mechanism of cytoplasmic SETDB1 in MBC and suggested that a CRM1 inhibitor may be a suitable option for patients with high cytoplasmic SETDB1 expression.

Acknowledgements

Not applicable.

Funding

The present study was supported by National Natural Science Foundation of China (grant no. 82103573), Shandong Provincial Natural Science Foundation, China (grant no. ZR2019BH047), Research Fund for Lin He's Academician Workstation of New Medicine and Clinical Translation in Jining Medical University (grant no. JYHL2018FZD07) and National Natural Cultivation Project of Jining Medical University (grant no. JYP2019KJ27).

Availability of data and materials

The data generated in the present study may be found in the Gene Expression Omnibus under accession number GSE253717 or at the following URL: https://www.ncbi.nlm.nih.gov/geo/query/acc.cgi?acc=GSE253717.

Authors' contributions

SH and SY conceived and designed the study. TW collected samples and patient information. WY, YW, TW, YX, XJ and HQ performed experiments and analyzed the data. SH, SY and WY wrote and revised the manuscript. SH and WY confirm the authenticity of all the raw data. All authors have read and approved the final manuscript.

Ethics approval and consent to participate

All primary BC samples were obtained from Affiliated Hospital of Jining Medical University under protocols approved by the Ethics Committee of Jining Medical University (approval no. 2021B090; Jining, China. Written informed consent was obtained from all patients.

Patient consent for publication

Not applicable.

Competing interests

The authors declare that they have no competing interests.

References

1. Sung H, Ferlay J, Siegel RL, Laversanne M, Soerjomataram I, Jemal A and Bray F: Global cancer statistics 2020: GLOBOCAN estimates of incidence and mortality worldwide for 36 cancers in 185 countries. CA Cancer J Clin 71: 209-249, 2021.
2. Hotton J, Lusque A, Leufflen L, Campone M, Levy C, Honart JF, Mailliez A, Debled M, Gutowski M, Leheurteur M, *et al*: Early locoregional breast surgery and survival in de novo metastatic breast cancer in the multicenter national ESME cohort. Ann Surg 277: e153-e161, 2023.
3. Wang H, An W, Cao R, Xia L, Erdjument-Bromage H, Chatton B, Tempst P, Roeder RG and Zhang Y: mAM facilitates conversion by ESET of dimethyl to trimethyl lysine 9 of histone H3 to cause transcriptional repression. Mol Cell 12: 475-487, 2003.

4. Schultz DC, Ayyanathan K, Negorev D, Maul GG and Rauscher FJ III: SETDB1: A novel KAP-1-associated histone H3, lysine 9-specific methyltransferase that contributes to HP1-mediated silencing of euchromatic genes by KRAB zinc-finger proteins. Genes Dev 16: 919-932, 2002.
5. Rodriguez-Paredes M, Martinez de Paz A, Simó-Riudalbas L, Sayols S, Moutinho C, Moran S, Villanueva A, Vázquez-Cedeira M, Lazo PA, Carneiro F, *et al*: Gene amplification of the histone methyltransferase SETDB1 contributes to human lung tumorigenesis. Oncogene 33: 2807-2813, 2014.
6. Cruz-Tapias P, Zakharova V, Perez-Fernandez OM, Mantilla W, RamÍRez-Clavijo S and Ait-Si-Ali S: Expression of the major and pro-oncogenic H3K9 lysine methyltransferase SETDB1 in non-small cell lung cancer. Cancers (Basel) 11: 1134, 2019.
7. Wong CM, Wei L, Law CT, Ho DW, Tsang FH, Au SL, Sze KM, Lee JM, Wong CC and Ng IO: Up-regulation of histone methyltransferase SETDB1 by multiple mechanisms in hepatocellular carcinoma promotes cancer metastasis. Hepatology 63: 474-487, 2016.
8. Fazio M, van Rooijen E, Mito JK, Modhurima R, Weiskopf E, Yang S and Zon LI: Recurrent co-alteration of HDGF and SETDB1 on chromosome 1q drives cutaneous melanoma progression and poor prognosis. Pigment Cell Melanoma Res 34: 641-647, 2021.
9. Ryu TY, Kim K, Kim SK, Oh JH, Min JK, Jung CR, Son MY, Kim DS and Cho HS: SETDB1 regulates SMAD7 expression for breast cancer metastasis. BMB Rep 52: 139-144, 2019.
10. Strepkos D, Markouli M, Klonou A, Papavassiliou AG and Piperi C: Histone methyltransferase SETDB1: A common denominator of tumorigenesis with therapeutic potential. Cancer Res 81: 525-534, 2021.
11. Liu L, Kimball S, Liu H, Holowatyj A and Yang ZQ: Genetic alterations of histone lysine methyltransferases and their significance in breast cancer. Oncotarget 6: 2466-2482, 2015.
12. Xiao JF, Sun QY, Ding LW, Chien W, Liu XY, Mayakonda A, Jiang YY, Loh XY, Ran XB, Doan NB, *et al*: The c-MYC-BMI1 axis is essential for SETDB1-mediated breast tumourigenesis. J Pathol 246: 89-102, 2018.
13. Regina C, Compagnone M, Peschiaroli A, Lena A, Annicchiarico-Petruzzelli M, Piro MC, Melino G and Candi E: Setdb1, a novel interactor of ΔNp63, is involved in breast tumorigenesis. Oncotarget 7: 28836-28848, 2016.
14. Zhang H, Cai K, Wang J, Wang X, Cheng K, Shi F, Jiang L, Zhang Y and Dou J: MiR-7, inhibited indirectly by lincRNA HOTAIR, directly inhibits SETDB1 and reverses the EMT of breast cancer stem cells by downregulating the STAT3 pathway. Stem Cells 32: 2858-2868, 2014.
15. Wu M, Fan B, Guo Q, Li Y, Chen R, Lv N, Diao Y and Luo Y: Knockdown of SETDB1 inhibits breast cancer progression by miR-381-3p-related regulation. Biol Res 51: 39, 2018.
16. Tachibana K, Gotoh E, Kawamata N, Ishimoto K, Uchihara Y, Iwanari H, Sugiyama A, Kawamura T, Mochizuki Y, Tanaka T, *et al*: Analysis of the subcellular localization of the human histone methyltransferase SETDB1. Biochem Biophys Res Commun 465: 725-731, 2015.
17. Cho S, Park JS and Kang YK: Regulated nuclear entry of over-expressed Setdb1. Genes Cells 18: 694-703, 2013.
18. Beyer S, Pontis J, Schirwis E, Battisti V, Rudolf A, Le Grand F and Ait-Si-Ali S: Canonical Wnt signalling regulates nuclear export of Setdb1 during skeletal muscle terminal differentiation. Cell Discov 2: 16037, 2016.
19. Guo J, Dai X, Laurent B, Zheng N, Gan W, Zhang J, Guo A, Yuan M, Liu P, Asara JM, *et al*: AKT methylation by SETDB1 promotes AKT kinase activity and oncogenic functions. Nat Cell Biol 21: 226-237, 2019.
20. Wang G, Long J, Gao Y, Zhang W, Han F, Xu C, Sun L, Yang SC, Lan J, Hou Z, *et al*: SETDB1-mediated methylation of Akt promotes its K63-linked ubiquitination and activation leading to tumorigenesis. Nat Cell Biol 21: 214-225, 2019.
21. Yang W, Su Y, Hou C, Chen L, Zhou D, Ren K, Zhou Z, Zhang R and Liu X: SETDB1 induces epithelial-mesenchymal transition in breast carcinoma by directly binding with Snail promoter. Oncol Rep 41: 1284-1292, 2019.
22. Livak KJ and Schmittgen TD: Analysis of relative gene expression data using real-time quantitative PCR and the 2(-Delta Delta C(T)) method. Methods 25: 402-408, 2001.
23. Hanahan D and Weinberg RA: Hallmarks of cancer: The next generation. Cell 144: 646-674, 2011.
24. DeBerardinis RJ and Chandel NS: Fundamentals of cancer metabolism. Sci Adv 2: e1600200, 2016.
25. Pavlova NN and Thompson CB: The emerging hallmarks of cancer metabolism. Cell Metab 23: 27-47, 2016.
26. Shim H, Dolde C, Lewis BC, Wu CS, Dang G, Jungmann RA, Dalla-Favera R and Dang CV: c-Myc transactivation of LDH-A: Implications for tumor metabolism and growth. Proc Natl Acad Sci USA 94: 6658-6663, 1997.
27. Shi MY, Wang Y, Shi Y, Tian R, Chen X, Zhang H, Wang K, Chen Z and Chen R: SETDB1-mediated CD147-K71 di-methylation promotes cell apoptosis in non-small cell lung cancer. Genes Dis 11: 978-992, 2023.
28. Kouzarides T: Chromatin modifications and their function. Cell 128: 693-705, 2007.
29. Dawson MA and Kouzarides T: Cancer epigenetics: From mechanism to therapy. Cell 150: 12-27, 2012.
30. Lee ST, Li Z, Wu Z, Aau M, Guan P, Karuturi RK, Liou YC and Yu Q: Context-specific regulation of NF-κB target gene expression by EZH2 in breast cancers. Mol Cell 43: 798-810, 2011.
31. Lehmann BD, Bauer JA, Chen X, Sanders ME, Chakravarthy AB, Shyr Y and Pietenpol JA: Identification of human triple-negative breast cancer subtypes and preclinical models for selection of targeted therapies. J Clin Invest 121: 2750-2767, 2011.
32. Tsusaka T, Shimura C and Shinkai Y: ATF7IP regulates SETDB1 nuclear localization and increases its ubiquitination. EMBO Rep 20: e48297, 2019.
33. Zheng Q, Cao Y, Chen Y, Wang J, Fan Q, Huang X, Wang Y, Wang T, Wang X, Ma J and Cheng J: Senp2 regulates adipose lipid storage by de-SUMOylation of Setdb1. J Mol Cell Biol 10: 258-266, 2018.
34. Liu S, Brind'Amour J, Karimi MM, Shirane K, Bogutz A, Lefebvre L, Sasaki H, Shinkai Y and Lorincz MC: Setdb1 is required for germline development and silencing of H3K9me3-marked endogenous retroviruses in primordial germ cells. Genes Dev 28: 2041-2055, 2014.
35. Collins PL, Kyle KE, Egawa T, Shinkai Y and Oltz EM: The histone methyltransferase SETDB1 represses endogenous and exogenous retroviruses in B lymphocytes. Proc Natl Acad Sci USA 112: 8367-8372, 2015.
36. Pasquarella A, Ebert A, Pereira de Almeida G, Hinterberger M, Kazerani M, Nuber A, Ellwart J, Klein L, Busslinger M and Schotta G: Retrotransposon derepression leads to activation of the unfolded protein response and apoptosis in pro-B cells. Development 143: 1788-1799, 2016.
37. Martin FJ, Xu Y, Lohmann F, Ciccone DN, Nicholson TB, Loureiro JJ, Chen T and Huang Q: KMT1E-mediated chromatin modifications at the FcγRIIb promoter regulate thymocyte development. Genes Immun 16: 162-169, 2015.
38. Takikita S, Muro R, Takai T, Otsubo T, Kawamura YI, Dohi T, Oda H, Kitajima M, Oshima K, Hattori M, *et al*: A histone methyltransferase ESET is critical for T cell development. J Immunol 197: 2269-2279, 2016.
39. Yizhak K, Le Dévédec SE, Rogkoti VM, Baenke F, de Boer VC, Frezza C, Schulze A, van de Water B and Ruppin E: A computational study of the Warburg effect identifies metabolic targets inhibiting cancer migration. Mol Syst Biol 10: 744, 2014.
40. Warburg O: On the origin of cancer cells. Science 123: 309-314, 1956.
41. Gao H, Yu Z, Bi D, Jiang L, Cui Y, Sun J and Ma R: Akt/PKB interacts with the histone H3 methyltransferase SETDB1 and coordinates to silence gene expression. Mol Cell Biochem 305: 35-44, 2007.
42. Liu T, Chen X, Li T, Li X, Lyu Y, Fan X, Zhang P and Zeng W: Histone methyltransferase SETDB1 maintains survival of mouse spermatogonial stem/progenitor cells via PTEN/AKT/FOXO1 pathway. Biochim Biophys Acta Gene Regul Mech 1860: 1094-1102, 2017.
43. Noh HJ, Kim KA and Kim KC: p53 down-regulates SETDB1 gene expression during paclitaxel induced-cell death. Biochem Biophys Res Commun 446: 43-48, 2014.
44. Chen K, Zhang F, Ding J, Liang Y, Zhan Z, Zhan Y, Chen LH and Ding Y: Histone methyltransferase SETDB1 promotes the progression of colorectal cancer by inhibiting the expression of TP53. J Cancer 8: 3318-3330, 2017.
45. Osaka N and Sasaki AT: Beyond Warburg: LDHA activates RAC for tumour growth. Nat Metab 4: 1623-1625, 2022.
46. Hou X, Shi X, Zhang W, Li D, Hu L, Yang J, Zhao J, Wei S, Wei X, Ruan X, *et al*: LDHA induces EMT gene transcription and regulates autophagy to promote the metastasis and tumorigenesis of papillary thyroid carcinoma. Cell Death Dis 12: 347, 2021.

47. Cai H, Li J, Zhang Y, Liao Y, Zhu Y, Wang C and Hou J: LDHA promotes oral squamous cell carcinoma progression through facilitating glycolysis and epithelial-mesenchymal transition. Front Oncol 9: 1446, 2019.
48. Herz HM, Garruss A and Shilatifard A: SET for life: Biochemical activities and biological functions of SET domain-containing proteins. Trends Biochem Sci 38: 621-639, 2013.
49. Van Duyne R, Easley R, Wu W, Berro R, Pedati C, Klase Z, Kehn-Hall K, Flynn EK, Symer DE and Kashanchi F: Lysine methylation of HIV-1 Tat regulates transcriptional activity of the viral LTR. Retrovirology 5: 40, 2008.
50. Fei Q, Shang K, Zhang J, Chuai S, Kong D, Zhou T, Fu S, Liang Y, Li C, Chen Z, *et al*: Histone methyltransferase SETDB1 regulates liver cancer cell growth through methylation of p53. Nat Commun 6: 8651, 2015.
51. Zhu H, Yang Y, Wang L, Xu X, Wang T and Qian H: Leptomycin B inhibits the proliferation, migration, and invasion of cultured gastric carcinoma cells. Biosci Biotechnol Biochem 84: 290-296, 2020.
52. Batham J, Lim PS and Rao S: SETDB-1: A potential epigenetic regulator in breast cancer metastasis. Cancers (Basel) 11: 1143, 2019.